Controlled growth of tetrapod-branched inorganic nanocrystals

LIBERATO MANNA[1,2], DELIA J. MILLIRON*[1], ANDREAS MEISEL*[1], ERIK C. SCHER[1] AND A. PAUL ALIVISATOS†[1]

[1]Department of Chemistry, University of California, Berkeley and Materials Sciences Division, Lawrence Berkeley National Laboratory, Berkeley, California 94720, USA
[2]Permanent address: National Nanotechnology Lab of INFM, Via Arnesano, 73100 Lecce, Italy
*These authors contributed equally to this work
†e-mail: alivis@uclink4.berkeley.edu

Published online: 25 May 2003; doi:10.1038/nmat902

Nanoscale materials are currently being exploited as active components in a wide range of technological applications in various fields, such as composite materials[1,2], chemical sensing[3], biomedicine[4–6], optoelectronics[7–9] and nanoelectronics[10–12]. Colloidal nanocrystals are promising candidates in these fields, due to their ease of fabrication and processibility. Even more applications and new functional materials might emerge if nanocrystals could be synthesized in shapes of higher complexity than the ones produced by current methods (spheres, rods, discs)[13–19]. Here, we demonstrate that polytypism, or the existence of two or more crystal structures in different domains of the same crystal, coupled with the manipulation of surface energy at the nanoscale, can be exploited to produce branched inorganic nanostructures controllably. For the case of CdTe, we designed a high yield, reproducible synthesis of soluble, tetrapod-shaped nanocrystals through which we can independently control the width and length of the four arms.

Polytypism is generally prevalent in open, tetrahedrally bonded structures, such as those occurring in the group IV, III-V and II-VI semiconductors[20–22]. Crystal structures of these and many other polytypic materials share a common crystal facet, which can be used to achieve branching. The ±{111} facets of the cubic (zinc blende) structure are atomically identical to the ±(0001) facets of the hexagonal (wurtzite) structure (Fig. 1). The most basic branched polytypic crystal that can therefore be produced using these materials is a 'tetrapod', consisting of a zinc-blende core with four {111} facets, each projecting a wurtzite rod terminated with the $(000\bar{1})$ facet. For such a structure to be formed, there must be a mechanism by which the stability of the two phases reverses during growth.

In conventional bulk crystal growth, some examples exist of controlled formation and growth of polytypic structures[20], and of modulated growth rates of different crystal facets as a function of time[23]. However, the advent of new methods for preparing inorganic nanocrystals with well-controlled sizes and elementary shapes provides a new set of tools that can be adapted to this purpose[13–19]. Tetrapod-shaped crystals with dimensions on the nanometre and micrometre scale have been observed in a variety of II-VI semiconductors[17,24–26], and a low yield of colloidal semiconductor tetrapods was observed in the syntheses of CdSe nanorods[27]. In a study of several different II-VI semiconductor materials, we have found that it is possible to obtain a high yield of colloidal semiconductor tetrapods with well-controlled nanoscale dimensions for the case of CdTe. A key parameter for achieving tetrapod growth is the energy difference between the wurtzite and the zinc-blende structures, which determines the temperature

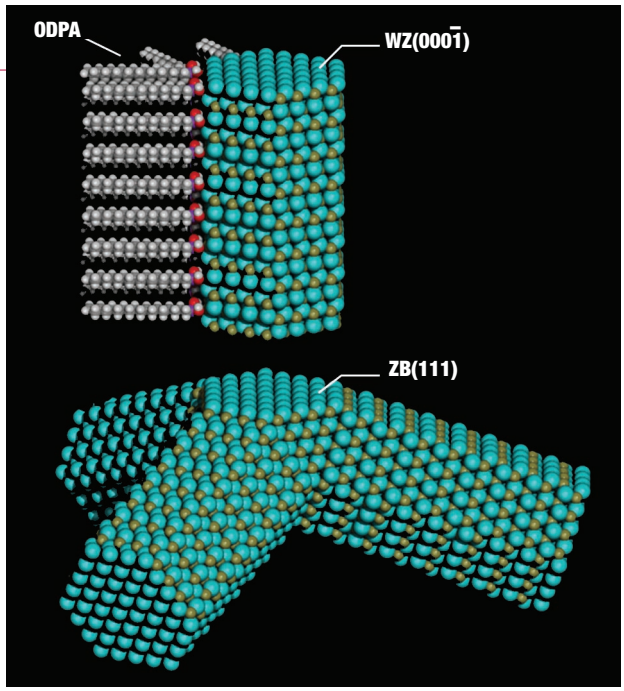

Figure 1 Proposed model of a CdTe tetrapod. The exploded view of one arm illustrates the identical nature of the (111) zinc blende (ZB) and $(000\bar{1})$ wurtzite (WZ) facets of the nucleus and the arms, respectively (Cd atoms are yellow, Te atoms are blue). Phosphonic acid molecules selectively bind to the lateral facets of the arms, as suggested in the figure (for clarity, only two facets are shown covered). High-resolution transmission electron microscope (HRTEM) analysis would further clarify the shape of the cubic nucleus and the relative orientations between the various arms of the tetrapod.

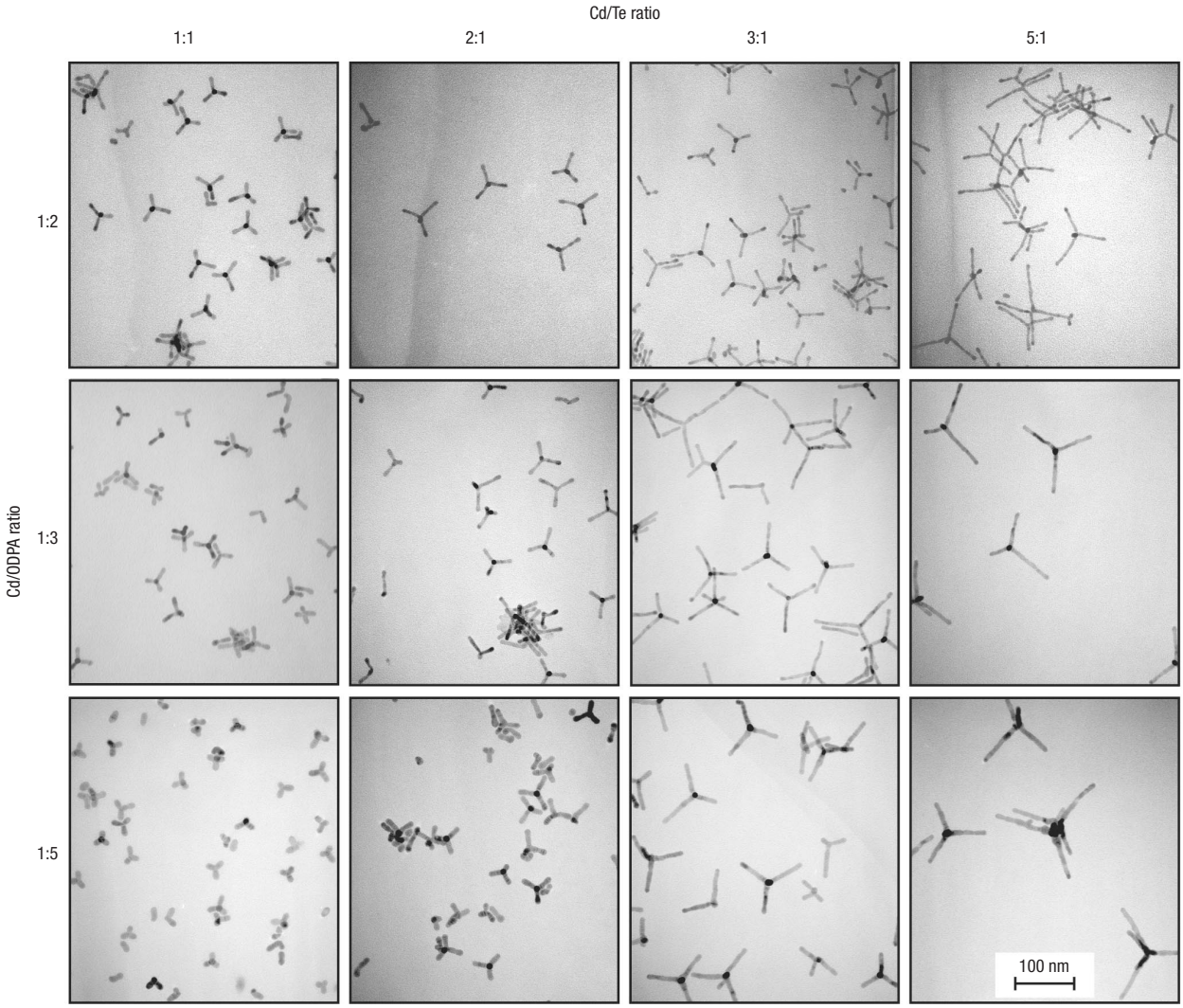

Figure 2 Electron microscopy images of CdTe tetrapods. TEMs of the CdTe tetrapods grown at various reaction conditions. The Cd/Te ratio was varied from 1:1 to 5:1, and the Cd/ODPA ratio was varied from 1:2 to 1:5 (the Cd/OPDA ratio must be 1:2 at maximum for the CdO to decompose completely). An increase in the Cd/Te ratio leads to tetrapods with longer arms, whereas higher Cd/ODPA ratios result in larger arm diameters. In all the experiments the amount of Te:TOP solution injected was adjusted with respect to the Cd/Te ratio. Also, the amount of ODPA added varied depending on the Cd/OPDA ratio. The total amount of TOPO + ODPA was always equal to 4 g. For the syntheses done at Cd/ODPA ratio of 1:2, the amount of CdO initially dissolved in the TOPO/ODPA mixture was 51 mg (1:1 Cd/Te), 102 mg (2:1 Cd/Te), and 153 mg (for both 3:1 and 5:1 Cd/Te), respectively. For the syntheses done at Cd/ODPA ratios of 1:3 and 1:5, the amount of CdO initially dissolved in the TOPO/ODPA mixture are 35 mg (1:1 Cd/Te) and 102 mg (for 2:1, 3:1 and 5:1 Cd/Te), respectively. Avoiding a large temperature drop after the injection of the Te:TOP solution is crucial to ensure both a faster recovery of the thermal equilibrium between the flask and the heating mantle and a higher homogeneity and reproducibility of the reaction conditions.

range in which one structure can be preferred during nucleation and the other during growth. In very ionic or very covalent cases, in which polytypism is rarely encountered, this difference can exceed 10 meV per atom[21], rendering it impractical to switch between the two growth modes during a reaction. In the case of CdS, CdSe and ZnS, the energy difference is only a few millielectronvolts per atom, and it is difficult to isolate controllably the growth of one phase at a time. CdTe represents an intermediate case, for which the energy difference between the two crystal structures is large enough that, even at the elevated temperatures preferred for high-quality wurtzite growth, nucleation can occur selectively in the zinc-blende structure. In CdTe, wurtzite growth is favoured by using higher temperatures in the presence of alkyl chain phosphonic acids[28]. These molecules are well known to stabilize selectively the non-polar lateral facets of hexagonal CdSe and CdTe nanocrystals[29,30], which have no equivalent in the cubic structure. This stabilization considerably reduces the growth rate of these facets[16,27]. Thus, the observation of high yields of CdTe tetrapods is consistent with nucleation in the zinc-blende phase, but growth of arms in the wurtzite phase, which is stabilized by alkyl phosphonic acids. Other materials with intermediate values of the zinc blende–wurtzite energy difference such as SiC, AlP, and others[21] might be similarly exploited to control branching.

Beyond control of the phase during nucleation and growth, manipulation of the growth kinetics enables independent tuning of the arm lengths and diameters. Figure 2 shows a series of transmission electron microscope (TEM) images of typical CdTe tetrapods of various

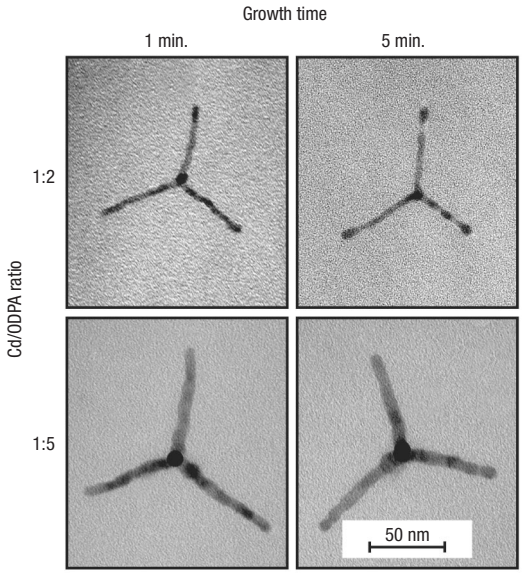

Figure 3 Time-dependent shape evolution of CdTe tetrapods. TEMs of CdTe tetrapods extracted from the same synthesis at 1 and at 5 minutes, respectively, for two syntheses carried out at the same Cd/Te ratio (5:1) but at two different Cd/ODPA ratios (1:2 and 1:5). There is no remarkable difference in the tetrapods extracted at 1 and at 5 minutes for the synthesis done at 1:5 Cd/ODPA ratio. On the other hand, the tetrapods extracted from the synthesis done at 1:2 Cd/ODPA ratio show significant ripening at their ends.

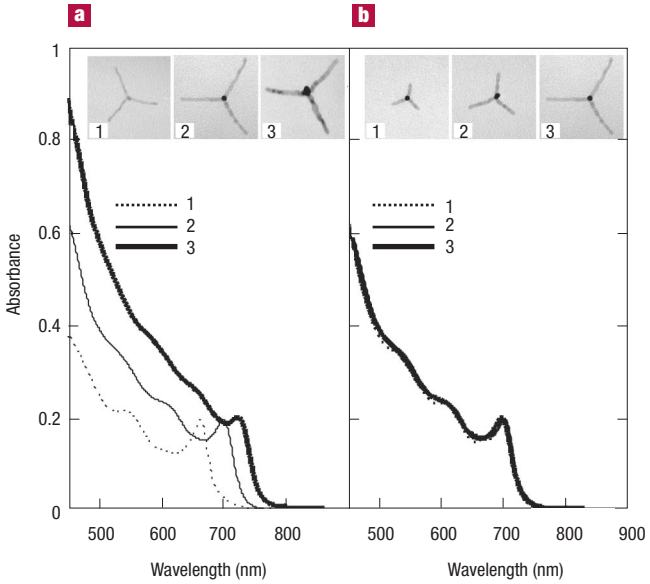

Figure 4 Influence of the shape of CdTe tetrapods on optical absorption spectra. Ensemble optical absorption spectra **a**, for a series of tetrapods having comparable arm lengths but different diameters, and **b**, for a series of tetrapods having comparable arm diameters but different lengths. The confinement energy is mainly dictated by the arm diameter.

lengths and aspect ratios, illustrating the influence of the main growth parameters on shape. We find that once the basic tetrapod shape is formed, growth of the arms occurs according to the controllable kinetic mechanisms previously observed for nanorods[27]. Higher Cd/Te ratios result in longer arms, whereas more n-octadecylphosphonic acid (ODPA) per Cd yields larger arm diameters. Anisotropy results from fast growth, and the growth rate is limited by the concentration of the Cd precursor, which is a strong complex between Cd^{2+} and phosphonic acid. Hence, higher Cd/Te ratios keep the reaction in the anisotropic growth regime for a longer time, leading to longer arms. On the other hand, the presence of more phosphonic acid per Cd (lower Cd/ODPA ratio) decreases the reactivity of the Cd precursor and so the driving force for its addition to the crystal[31], thereby slowing the growth rate for a given Cd concentration. However, the growth of the arms continues as long as the Cd concentration is sufficiently high. This results in less anisotropic rods, with a larger diameter for a given length.

A further consequence of the kinetically controlled growth appears in the shape evolution of tetrapods beyond the anisotropic growth regime. In Fig. 3, we compare CdTe tetrapods extracted from the same synthesis, at 1 and at 5 minutes, respectively, for two syntheses carried out at the same Cd/Te ratio but at two different Cd/ODPA ratios. In both cases, most of the anisotropic growth takes place in the first minute after injection, when the concentration of monomers is high. The facet growing most quickly during this period is the one with the highest interfacial energy. However, when the concentration of monomer drops, this facet is also the one that starts dissolving first. For instance, at high (1:2) Cd/ODPA ratio, the tetrapods grown for 5 minutes have distinctly rounded ends. The dissolution of the end of an arm (the unstable $(000\bar{1})$ facet) leads to the local formation of more thermodynamically stable facets (anisotropic Ostwald ripening). This results in round ends of larger diameter on the arms. This effect is not apparent in the sample grown at a lower (1:5) Cd/ODPA ratio, because a slower growth rate delays the Ostwald ripening regime to longer times.

A remarkable feature of the synthesis reported here is that the four arms of the tetrapod are equal in length to within a few percent. These structures are obtained in yields as high as 70%. This is consistent with a zinc-blende nucleation that occurs early in time, followed by a period of growth in which the wurtzite phase is favoured by selective adhesion of the phosphonic acid surfactant. However, tripod, dipod and monopod or rod-shaped crystals are also obtained, albeit in much lower yields. These structures might arise if all four facets of the zinc-blende nucleus are not identical when the growth period sets in. The alternative possibility, that rod-shaped nanocrystals attach to each other, appears to be inconsistent with our results, based on the fact that we do not see the tetrapod yield increase at longer growth times. In the very long time limit of Ostwald ripening, arm lengths are observed to vary more, presumably because an arm that is even slightly larger than the others can consume the smaller ones. The yields of 70% can potentially be further improved by post-synthesis purification by selective precipitation.

Tetrapod nanocrystals display a higher degree of solubility compared with separate rods of the same length and diameter as the arms. This can be explained by the fact that two rods can more readily achieve a large contact area with each other in solution than can two tetrapods; such contact can lead to aggregation. This is reminiscent of the reason why organic dendrimers are more soluble than comparable molecular weight linear polymers. Indeed, there are numerous points of analogy between organic dendrimers and the inorganic tetrapods reported here, which can be thought of as first-generation inorganic dendrimers. In the future it may be possible to reliably make higher generation inorganic dendrimers by temperature cycling, because lower temperatures favour the zinc-blende structure. The enhanced

solubility of the tetrapods means that they can be processed into devices more readily.

The tetrapod shape can potentially lead to a variety of interesting mechanical, electrical and optical properties. For example, due to their three-dimensional character, tetrapods may be important alternatives to fibres and rods as additives for mechanical reinforcement of polymers. As a good example of the optical properties, we compare the electronic absorption spectra for two series of tetrapod samples having different arm lengths and diameters (Fig. 4). In a rod or in a tetrapod-shaped nanocrystal, most of the confinement energy is along the diameter of the hexagonal arms[32]. Tetrapods having comparable arm lengths but different diameters in fact show remarkable differences in their bandgap energy (Fig. 4a), whereas spectra of tetrapods with comparable diameters but different arm lengths are almost identical (Fig. 4b). This independent tunability of the arm length and the bandgap is very attractive for nanocrystal-based solar cells. The inherent property of a tetrapod to self-align on a substrate with one arm always pointing towards one electrode, combined with the low bandgap of CdTe, should substantially enhance the device efficiencies of the reported hybrid nanorod–polymer solar cells[8].

METHODS

MATERIALS

Cadmium oxide (CdO) (99.99+%), tellurium (Te) (99.8%, 200 mesh), and tri-n-octylphosphine oxide ($C_{24}H_{51}OP$ or TOPO, 99%) were purchased from Aldrich. n-Octadecylphosphonic acid ($C_{18}H_{39}O_3P$ or ODPA, 99 %) was purchased from Oryza Laboratories (now Polycarbon Industries, Devens, Massachusetts, USA). Trioctylphosphine (TOP) (90 %) was purchased from Fluka. All solvents used were anhydrous, purchased from Aldrich, and used without any further purification.

SYNTHESIS OF CDTE TETRAPODS

All manipulations were performed using standard air-free techniques. The Te precursor solution was prepared by dissolving tellurium powder in TOP (concentration of Te 10 wt%). The mixture was stirred for 30 minutes at 250 °C, then cooled and centrifuged to remove any remaining insoluble particles. In a typical synthesis of CdTe tetrapods, a mixture of ODPA, TOPO and CdO was degassed at 120 °C for 20 minutes in a 50 ml three-neck flask connected to a Liebig condenser. The mixture was heated slowly under argon until the CdO decomposed and the solution turned clear and colourless. Next, 1.5 g of TOP was added and the temperature was further raised to 320 °C. After that the Te:TOP precursor solution was injected quickly. The temperature dropped to 315 °C and was maintained at this value throughout the synthesis. All syntheses were stopped after 5 minutes by removing the heating mantle and by rapidly cooling the flask. After cooling the solution to 70 °C, 3–4 ml anhydrous toluene were added to the flask, and the dispersion was transferred to an argon drybox. The minimum amount of anhydrous methanol, which was required to cause the precipitation of the nanocrystals after centrifugation, was added to the dispersion. In this way, we prevented potential co-precipitation of the Cd-phosphonate complex. After removing the supernatant, the precipitate was re-dissolved twice in toluene, re-precipitated with methanol and stored in the drybox. The resulting tetrapods are obtained in high yield, and they are soluble in common organic solvents, such as toluene and chloroform. For the syntheses reported in this paper, the Cd/Te molar ratio was varied from 1:1 to 5:1, and the Cd/ODPA molar ratio was varied from 1:2 to 1:5.

SAMPLE CHARACTERIZATION

The structure and size of the CdTe nanocrystals were measured by using TEM. At the UC Berkeley Electron Microscope Lab, a FEI Tecnai 12 electron microscope was used. The microscope was operated at an accelerating voltage of 100 kV. To evaluate the growth kinetics of the syntheses, a small amount of the sample (~0.1 ml) was removed by syringe from the flask every minute and mixed into anhydrous toluene. The aliquots were transferred to the drybox and washed once with methanol according to the procedure described above. The precipitated nanocrystals were re-dissolved in toluene and deposited from dilute solution onto a film 3–4 nm thick of amorphous carbon supported by 400 mesh copper grids (purchased from Ted Pella, Redding, California, USA). One drop of nanocrystal solution in toluene was deposited onto the grid and evaporated. Ultraviolet–visible absorption spectra were measured using a Hewlett-Packard 8453 UV-visible diode array spectrometer equipped with a deuterium lamp having a resolution of 1.0 nm.

Received 21 November 2003; accepted 8 April 2003; published 25 May 2003.

References

1. Morris, C. A., Anderson, M. L., Stroud, R. M., Merzbacher, C. I. & Rolison, D. R. Silica sol as a nanoglue: Flexible synthesis of composite aerogels. *Science* **284,** 622–624 (1999).
2. Caruso, F. Hollow capsule processing through colloidal templating and self-assembly. *Chem. Europ. J.* **6,** 413–419 (2000).
3. Kong, J. *et al.* Nanotube molecular wires as chemical sensors. *Science* **287,** 622–625 (2000).
4. Bruchez, M., Moronne, M., Gin, P., Weiss, S. & Alivisatos, A. P. Semiconductor nanocrystals as fluorescent biological labels. *Science* **281,** 2013–2016 (1998).
5. Chan, W. C. W. & Nie, S. M. Quantum dot bioconjugates for ultrasensitive nonisotopic detection. *Science* **281,** 2016–2018 (1998).
6. Taton, T. A., Mirkin, C. A. & Letsinger, R. L. Scanometric DNA array detection with nanoparticle probes. *Science* **289,** 1757–1760 (2000).
7. Colvin, V. L., Schlamp, M. C. & Alivisatos, A. P. Light-emitting diodes made from cadmium selenide nanocrystals and a semiconducting polymer. *Nature* **370,** 354–357 (1994).
8. Huynh, W. U., Dittmer, J. J. & Alivisatos, A. P. Hybrid nanorod-polymer solar cells. *Science* **295,** 2425–2427 (2002).
9. Klimov, V. I. *et al.* Optical gain and stimulated emission in nanocrystal quantum dots. *Science* **290,** 314–317 (2000).
10. Fuhrer, M. S. *et al.* Crossed nanotube junctions. *Science* **288,** 494–497 (2000).
11. Duan, X. F., Huang, Y., Cui, Y., Wang, J. F. & Lieber, C. M. Indium phosphide nanowires as building blocks for nanoscale electronic and optoelectronic devices. *Nature* **409,** 66–69 (2001).
12. Gudiksen, M. S., Lauhon, L. J., Wang, J., Smith, D. & Lieber, C. M. Growth of nanowire superlattice structures for nanoscale photonics and electronics. *Nature* **415,** 617–620 (2002).
13. Murray, C. B., Norris, D. J. & Bawendi, M. G. Synthesis and characterization of nearly monodisperse CdE (E = S, Se, Te) semiconductor nanocrystallites. *J. Am. Chem. Soc.* **115,** 8706–8715 (1993).
14. Ahmadi, T. S., Wang, Z. L., Green, T. C., Henglein, A. & El-Sayed, M. A. Shape-controlled synthesis of colloidal platinum nanoparticles. *Science* **272,** 1924–1926 (1996).
15. Yu, Y. Y., Chang, S., Lee, C. J. & Wang, C. R. C. Gold nanorods: electrochemical synthesis and optical properties. *J. Phys. Chem. B* **101,** 6661–6664 (1997).
16. Peng, X. G. *et al.* Shape control of CdSe nanocrystals. *Nature* **404,** 59–61 (2000).
17. Jun, Y. W., Lee, S. M., Kang, N. J. & Cheon, J. Controlled synthesis of multi-armed CdS nanorod architectures using monosurfactant system. *J. Am. Chem. Soc.* **123,** 5150–5151 (2001).
18. Shevchenko, E. *et al.* Colloidal crystals of monodisperse FePt nanoparticles grown by a three-layer technique of controlled oversaturation. *Adv. Mater.* **14,** 287–290 (2002).
19. Ni, Y. H., Ge, X. W., Zhang, Z. C. & Ye, Q. Fabrication and characterization of the plate-shaped gamma-Fe_2O_3 nanocrystals. *Chem. Mater.* **14,** 1048–1052 (2002).
20. Park, C. H., Cheong, B. H., Lee, K. H. & Chang, K. J. Structural and electronic properties of cubic, 2H, 4H, and 6H SiC. *Phys. Rev. B* **49,** 4485–4493 (1994).
21. Yeh, C. Y., Lu, Z. W., Froyen, S. & Zunger, A. Zinc-blende-wurtzite polytypism in semiconductors. *Phys. Rev. B* **46,** 10086–10097 (1992).
22. Ito, T. Simple criterion for wurtzite-zinc-blende polytypism in semiconductors. *Jpn J. Appl. Phys. Part 2* **37,** L1217–L1220 (1998).
23. Mason, B. J. Snow crystals, natural and man-made. *Contemp. Phys.* **33,** 227–243 (1992).
24. Jun, Y. W., Jung, Y. Y. & Cheon, J. Architectural control of magnetic semiconductor nanocrystals. *J. Am. Chem. Soc.* **124,** 615–619 (2002).
25. Chen, M. *et al.* Synthesis of rod-, twinrod-, and tetrapod-shaped CdS nanocrystals using a highly oriented solvothermal recrystallization technique. *J. Mater. Chem.* **12,** 748–753 (2002).
26. Dai, Y., Zhang, Y., Li, Q. K. & Nan, C. W. Synthesis and optical properties of tetrapod-like zinc oxide nanorods. *Chem. Phys. Lett.* **358,** 83–86 (2002).
27. Manna, L., Scher, E. C. & Alivisatos, A. P. Synthesis of soluble and processable rod-, arrow-, teardrop-, and tetrapod-shaped CdSe nanocrystals. *J. Am. Chem. Soc.* **122,** 12700–12706 (2000).
28. Bandaranayake, R. J., Wen, G. W., Lin, J. Y., Jiang, H. X. & Sorensen, C. M. Structural phase-behavior in II-VI semiconductor nanoparticles. *Appl. Phys. Lett.* **67,** 831–833 (1995).
29. Peng, Z. A. & Peng, X. G. Formation of high-quality CdTe, CdSe, and CdS nanocrystals using CdO as precursor. *J. Am. Chem. Soc.* **123,** 183–184 (2001).
30. Peng, Z. A. & Peng, X. G. Mechanisms of the shape evolution of CdSe nanocrystals. *J. Am. Chem. Soc.* **123,** 1389–1395 (2001).
31. Peng, Z. A. & Peng, X. G. Nearly monodisperse and shape-controlled CdSe nanocrystals via alternative routes: Nucleation and growth. *J. Am. Chem. Soc.* **124,** 3343–3353 (2002).
32. Li, L. S., Hu, J. T., Yang, W. D. & Alivisatos, A. P. Band gap variation of size- and shape-controlled colloidal CdSe quantum rods. *Nano Lett.* **1,** 349–351 (2001).

Acknowledgements

This work was supported by the Director, Office of Science, Office of Basic Energy Sciences, Division of Materials Sciences and Engineering, of the US Department of Energy under Contract No. DE-AC03-76SF00098 and by Grant No. 066995 through the University of Southern California, under prime sponsor DOD Advanced Research Projects Agency. D.S.M. gratefully acknowledges fellowship support from the US department of Defense. We would like to thank R. Zalpuri and G. Vrdoljak at the UC Berkeley Electron Microscope Lab for their assistance and the use of their TEM. We thank J. W. Jun and M. F. Casula for beneficial discussions.

Correspondence and requests for materials should be addressed to A.P.A.

Competing financial interests

The authors declare that they have no competing financial interests.